Journal of Physics: Conference Series **293** (2011) 012009 doi:10.1088/1742-6596/293/1/012009

Electromagnetic calorimeters of the CMD-3 detector

Denis Epifanov [1]

Budker Institute of Nuclear Physics
Academician Lavrentiev Avenue 11, Novosibirsk, 630090, Russia

E-mail: D.A.Epifanov@inp.nsk.su

Abstract.

Recently the CMD-3 detector has started to record the experimental information produced at the VEPP-2000 e^+e^- collider at BINP (Novosibirsk). CMD-3 is a general purpose detector for a study of e^+e^- annihilation to hadrons in the wide center-of-mass energy range, $\sqrt{s} = 0.3 \div 2$ GeV. The calorimetry in the detector is based on three subsystems: closest to the beam pipe barrel liquid xenon calorimeter, outer barrel calorimeter based on CsI scintillation crystals and endcap calorimeter made of BGO scintillation crystals. Construction and tests of the calorimeters are described, first results from the experimental runs are presented.

1. Introduction

The new electron-positron collider VEPP-2000 [1, 2] is operating now at Budker Institute of Nuclear Physics. Using round beam technique the collider will provide the luminosity up to 10^{32} cm^{-2}s^{-1} at the maximum center-of-mass (c.m.) energy $\sqrt{s} = 2$ GeV. The physical program includes a measurement of the $e^+e^- \to$ hadrons cross section in the wide c.m. energy range up to 2 GeV [3], a study of known and search for new vector mesons, study of $n\bar{n}$ and $p\bar{p}$ production cross sections in the vicinity of the threshold and search for exotic hadrons. It requires a detector with high efficiency for multiparticle events and good energy and angular resolutions for charged particles as well as for photons.

At present, two detectors, SND (Spherical Neutral Detector) [4] and CMD-3 (Cryogenic Magnetic Detector) [5, 6], are installed in two interaction regions of the collider. CMD-3 is a general purpose detector, its layout is shown in Fig. 1. The tracking system consists of a drift chamber [7] and two layers of a proportional Z-chamber inside a thin superconducting solenoid with 1.35 T magnetic field. The calorimetry in the detector is based on three subsystems: closest to the beam pipe barrel liquid xenon calorimeter (LXe) [8], outer barrel calorimeter based on the CsI scintillation crystals [9] and endcap calorimeter made of BGO scintillation crystals [10]. The detector is also equipped with a barrel-like arrangement of time-of-flight scintillation counters [11], located between LXe and CsI calorimeters, and muon-range system.

The main tasks of the calorimeter are: precise measurement of energy and coordinates of photons in the wide energy range $E_\gamma = 10$ MeV -1 GeV, the electron-hadron separation and generation of the fast signals for the neutral trigger of the CMD-3 detector.

[1] on behalf of the CMD-3 collaboration

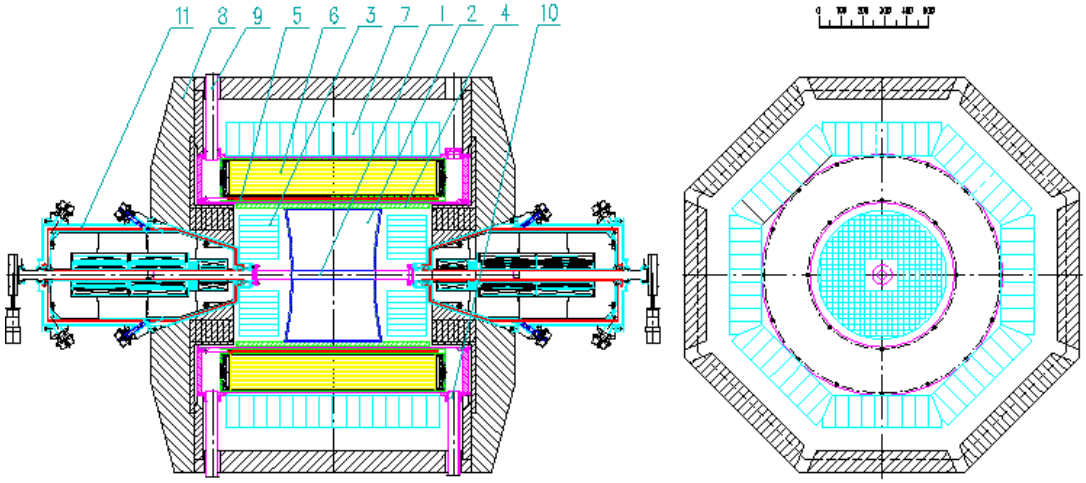

Figure 1. CMD-3 detector layout: 1 - vacuum chamber, 2 - drift chamber (DC), 3 - BGO endcap calorimeter (BGO), 4 - Z-chamber (ZC), 5 - superconducting solenoid, 6 - liquid Xe calorimeter(LXe), 7 - CsI barrel calorimeter (CsI), 8 - iron yoke, 9 - liquid He supply, 10 - vacuum pumpdown, 11 - VEPP-2000 superconducting magnetic lenses.

2. LXe calorimeter

The LXe barrel calorimeter contains 400 l of LXe (1200 kg) and has a depth of 15 cm that corresponds to $5X_0$, where X_0 is the radiation length. The total radiation thickness of the barrel part ($5X_0$(LXe)+$8X_0$(CsI)) is equal to $13X_0$. The LXe calorimeter covers polar angles from 38° to 142° with a solid angle of about $0.79\times4\pi$. To reduce the thickness of passive materials in front of the calorimeter down to the $0.38X_0$, both the LXe calorimeter and a superconducting solenoid are placed inside the common vacuum vessel. The working temperature of the calorimeter is 170 K with a xenon pressure of 1.4 atm.

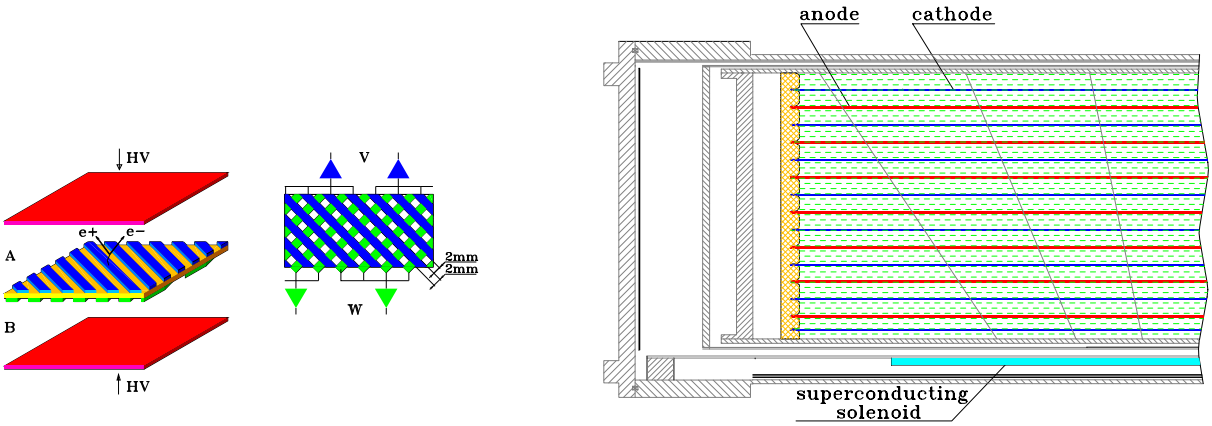

Figure 2. Design of electrodes of the LXe calorimeter

The LXe calorimeter consists of a set of ionization chambers with 7 cylindrical cathodes and 8 anodes, see Fig. 2. The electrodes were made of copper-plated G-10. Both conductive surfaces of the cathode electrodes are divided into strips. A set of four strips is connected to one superstrip read by one channel of electronics, as shown in Fig. 2. The width of the superstrips varies from 10.8 to 15.2 mm depending on the layer number. An induced charge is integrated for

4.5 μs (that is the time required for collection of electrons in an electric field of 1.5 kV/cm) and is used for the measurements of the photon conversion point coordinates and energy losses of the charged particles. Conductive surfaces of anode electrodes are divided into rectangular pads forming towers oriented to the interaction point. The induced current is integrated for 0.4 μs and then used to measure the energy deposition as well as provides signals for the neutral trigger of the detector. The total numbers of superstrips and towers are 2124 and 264, respectively. There are 33 rows of the towers along the beam direction with 8 towers in each row.

Each channel of the electronics includes a charge-sensitive preamplifier (CSP), a shaping amplifier and ADC. The shaping amplifier and ADC of the cathode channel are mounted on one Amplifier-Shaper-Digitizer board, which will be described in the next section. The circuit designs of the anode and cathode channels are similar. They differ only in terms of some active parts and time constants of the shaping RC-CR circuits. The equivalent input noise charge (ENC) of the anode preamplifier is about 3000 el. with an input capacitance of 500 pF. The ENC of the cathode CSP is about 2200 el. with an input capacitance of 1000 pF. The sensitivity of the anode channel is about 13500 el/MeV, while the typical amplitude from the cathode channel, measured with the cosmic ray particles, is about 36000 el.

The LXe calorimeter was installed in the detector and its parameters were studied with help of the cosmic-ray particles. The performed tests showed good stability of the electronics and expected level of the electronic noise. The spatial resolution varies from 0.7 to 1.4 mm depending on the layer number, in particular, because the strip capacitance increases from 400 pF to 700 pF.

3. CsI calorimeter

The CsI calorimeter consists of 8 octants, located around the LXe calorimeter, and contains 1152 counters with the total mass of crystals of about 2.8 tons. Each octant contains 9 linear modules oriented along the beam axis. Seven central modules of each octant consist of rectangular crystals, while two side modules are assembled from the crystals of special shape to avoid gaps between octants. Each module is assembled of 16 CsI crystals fixed on the steel framework to organize a linear array of 16 counters. The layout of the counter is shown in Fig. 3. It is based

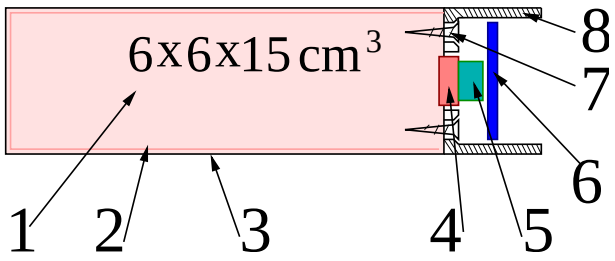

Figure 3. The layout of the CsI counter: 1 - crystal, 2 - porous teflon, 3 - aluminized lavsan, 4 - photodiode, 5 - rubber packing, 6 - preamplifier board, 7 - screws, 8 - steel framework.

on a CsI(Tl) or CsI(Na) crystal (1) of $6 \times 6 \times 15$ cm^3 size. To increase the scintillation light collection, it is wrapped with a layer of 200 μm thick porous teflon (2) and covered by the 20 μm thick aluminised mylar (3) to isolate a crystal from the external light. The scintillation light readout is performed by a Hamamatsu S2744-08 silicon PIN photodiode (4) with a sensitive area of 1×2 cm^2. Charge from the photodiode is converted to the voltage signal by the low noise charge sensitive preamplifier (6), attached to the photodiode. The electronic channel scheme is shown in Fig. 4. Signals from the preamplifiers come to the 32-channel Amplifier-Shaper-Digitizer board (ASD-32) via the twisted pairs. These boards are used to process signals in all calorimeters of the CMD-3. In the spectrometric part of the ASD-32 the amplification, shaping and amplitude digitization of the signal are performed. Digitized amplitudes are stored in the

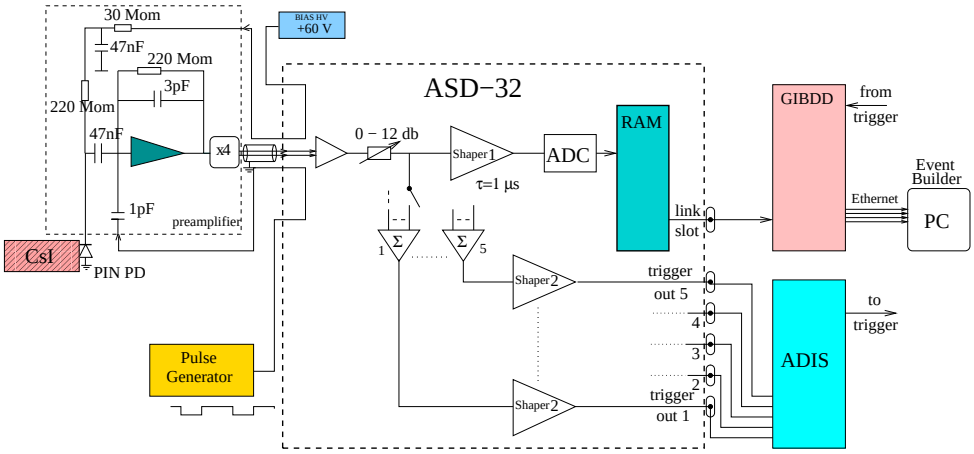

Figure 4. Scheme of the electronic channel.

on-line storage of the board, from which they are transferred to the online PC-farm through the special interface board [12]. The ASD-32 also forms fast analog sum signals to use them in the neutral trigger of the detector. The average noise over all channels is about 700 electrons and the sensitivity varies from about 2500 el./MeV for the CsI(Na)-counters to 5000 el./MeV for the CsI(Tl)-counters.

The calibration coefficients converting the ADC counts to energy are determined with help of cosmic-ray particles.

4. BGO calorimeter

The endcap calorimeter consists of two identical endcaps, each comprising 340 crystals. It covers the polar-angle regions from 16° to 49° and from 131° to 164°, the corresponding solid angle being $0.3\times4\pi$ sr. The length of each crystal is 150 mm, which corresponds to $13.4X_0$. The crystal transverse dimensions of 25×25 mm^2 were chosen on the basis of optimizing the calorimeter spatial resolution and the number of electronics channels. All crystal faces were polished, and light readout was accomplished on the basis of total internal reflection.

To simplify the mechanical structure of the endcap calorimeter and facilitate assembling, crystals were combined into blocks. The calorimeter was assembled from blocks of two types: 116 blocks of four crystals and 36 blocks of six crystals. Each block is equipped with PIN photodiodes with a sensitive area of 1 cm^2 and a board of charge-sensitive preamplifiers. The average noise over all channels is about 450 electrons and the sensitivity is about 500 el./MeV. The structure of a four-crystal block is shown in Fig. 5. In each endcap of the calorimeter, the blocks are mounted vertically on special supports into a copper ring of inner diameter 576 mm. The ring is fixed at the endface iron of the magnet yoke by means of four stainless-steel brackets.

The light output of BGO crystals decreases by about 1.5% as the temperature increases by 1°C. Since the crystal light output increases and the electronic noise decreases with temperature decrease, it is advantageous to work at low temperatures. A thermal-stabilization system allows us to maintain the temperature of the endcap calorimeter at the level of 10-12°C with long term stability better than 1°C.

The tests and calibration of the channels were carried out via accumulating spectra of the energy deposition caused by the propagation of cosmic-ray muons. For each crystal the spectrum of energy deposition is approximated by a Landau distribution function in the peak region. The value obtained in this way corresponds to the most probable energy release of 22.7 MeV, determined from a simulation. In this procedure the conversion coefficients from ADC channel

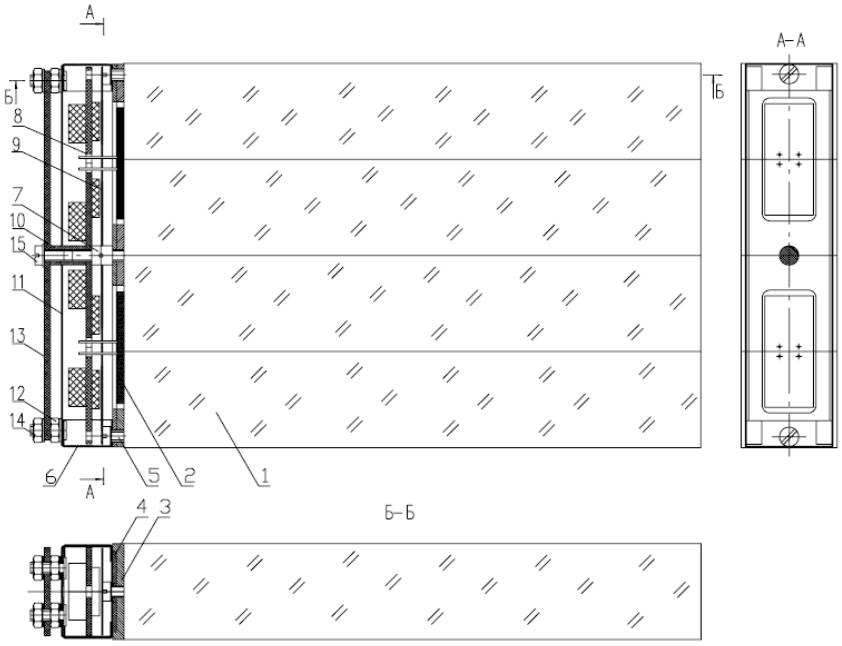

Figure 5. Layout of the four-crystal block: 1 - crystals, 2 - photodiodes, 3 - brass base plate, 4 - brass insertion plate, 5 - 3 screws, 6 - end caps, 7 - pin, 8 - preamplifier, 9 - insulator, 10 - bushing nut, 11 - side lits, 12 - nut, 13 - rear cap, 14 - nut, 15 - 5 screws.

to the deposited energy are calculated.

5. Neutral trigger system

Signals from all calorimeters are used in the neutral trigger system of the CMD-3 [13, 14]. To this end, channels of each calorimeter are combined in a certain number of trigger cells (TC): 80 TC in the LXe, 80 TC in the CsI and 48 TC in the BGO calorimeter. Analog signals from the TC are processed by 14 boards of the amplitude discriminators and summators (ADIS). ADIS boards digitize fast analog signals and generate logic signals for a cluster-finding module, which makes a decision and generates a start signal for data acquisition (DAQ) [12].

6. First results

Data taking with the completely assembled CMD-3 detector started in the first half of 2010. All calorimeters showed good performance, only a few dead channels were found. High stability of the DAQ system allowed us to record a data sample with the integrated luminosity of about 1.5 pb^{-1}. Figure 6(a) shows experimental events with two collinear tracks at the c.m. energy $\sqrt{s} = 1514$ MeV on the two-dimensional plot: total energy deposition in the LXe+CsI calorimeter versus momentum of the charged particle in DC. While signals from the cosmic-ray particles are suppressed by selection criteria, clearly seen are events of e^+e^- elastic scattering (Bhabha), $e^+e^- \to \mu^+\mu^-$ and events of beam interactions with the residual gas. Figure 6(b) demonstrates a distribution of the energy deposition in one endcap of the BGO calorimeter for the experimental events at the c.m. energy $\sqrt{s} = 1900$ MeV. One can see a clear peak coming from the Bhabha and $e^+e^- \to \gamma\gamma$ events producing electromagnetic showers in the BGO.

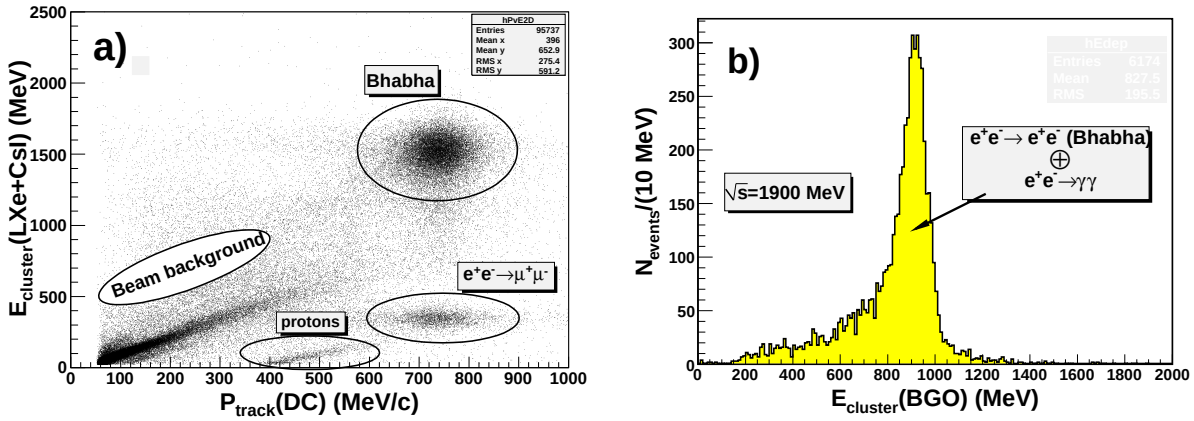

Figure 6. (a) Total energy deposition in the LXe+CsI calorimeter versus momentum of the charged particle in DC for the experimetal data collected at the c.m. energy $\sqrt{s} = 1514$ MeV. (b) Energy deposition in one endcap of the BGO calorimeter for the experimental events at the c.m. energy $\sqrt{s} = 1900$ MeV.

7. Conclusion

All calorimeters are installed in the CMD-3 detector. Their electronics is integrated in the DAQ system. The first data taking session showed good performance of the calorimeters. Monitoring of the calorimeters channels with the use of the generator calibration signal showed long term stability of the DAQ electronics. Energy calibration is done with help of the cosmic-ray muons. Work on the absolute energy calibration of the entire calorimeter with Bhabha events is in progress. A neutral trigger system is tested and will be included in DAQ soon.

8. Acknowledgments

This work was supported in part by Russian Federal Program "Scientific and scientific-pedagogical personnel of innovative Russia in 2009-2013".

References

[1] Yu. M. Shatunov *et al.*, *Prepared for 7th European Particle Accelerator Conference (EPAC 2000), Vienna, Austria, 26-30 Jun 2000*
[2] Yu. M. Shatunov, Phys. Part. Nucl. Lett. **5** (2008) 566.
[3] S. Eidelman, Nucl. Phys. Proc. Suppl. **162** (2006) 323.
[4] M. N. Achasov *et al.*, Nucl. Instrum. Meth. A **598** (2009) 31.
[5] V. M. Aulchenko *et al.*, "CMD-2M detector project. (In Russian)," BUDKER-INP-2001-45.
[6] G. V. Fedotovich [CMD-3 Collaboration], Nucl. Phys. Proc. Suppl. **162** (2006) 332.
[7] F. Grancagnolo *et al.*, Nucl. Instrum. Meth. A **598** (2009) 105.
[8] A. V. Anisyonkov *et al.*, Nucl. Instrum. Meth. A **598** (2009) 266.
[9] V. M. Aulchenko *et al.*, "Electromagnetic calorimeter based on the CsI scintillation crystals for the CMD-3 detector. (In Russian)," BUDKER-INP-2008-39.
[10] R. R. Akhmetshin, D. N. Grigoriev, V. F. Kazanin, S. M. Tsaregorodtsev and Yu. V. Yudin, Phys. Atom. Nucl. **72** (2009) 477 [Yad. Fiz. **72** (2009) 512].
[11] D. A. Drozhzhin *et al.*, Nucl. Instrum. Meth. A **598** (2009) 203.
[12] A. Ruban, A. Aulchenko, K. Kakhuta, A. Kozyrev, A. Selivanov, V. Titiov and Yu. Yudin, Nucl. Instrum. Meth. A **598** (2009) 317.
[13] K. I. Kakhuta, A. N. Kozyrev, A. A. Ruban and Yu. V. Yudin, Phys. Atom. Nucl. **72** (2009) 647 [Yad. Fiz. **72** (2009) 687].
[14] A. N. Kozyrev, A. A. Ruban and Yu. V. Yudin, Nucl. Instrum. Meth. A **598** (2009) 345.